# Bulk Superconductivity and Role of Fluctuations in the Iron-Based Superconductor FeSe at High Pressures

Elena Gati,[1,2,*] Anna E. Böhmer,[1,2,†] Sergey L. Bud'ko,[1,2] and Paul C. Canfield[1,2]
[1]*Ames Laboratory, U.S. Department of Energy, Iowa State University, Ames, Iowa 50011, USA*
[2]*Department of Physics and Astronomy, Iowa State University, Ames, Iowa 50011, USA*

(Received 4 June 2019; published 16 October 2019)

The iron-based superconductor FeSe offers a unique possibility to study the interplay of superconductivity with purely nematic as well magnetic-nematic order by pressure ($p$) tuning. By measuring specific heat under $p$ up to 2.36 GPa, we study the multiple phases in FeSe using a thermodynamic probe. We conclude that superconductivity is bulk across the entire $p$ range and competes with magnetism. In addition, whenever magnetism is present, fluctuations exist over a wide temperature range above both the bulk superconducting and the magnetic transitions. Whereas the magnetic fluctuations are likely temporal, the superconducting fluctuations may be either temporal or spatial. These observations highlight similarities between FeSe and underdoped cuprate superconductors.

DOI: 10.1103/PhysRevLett.123.167002

FeSe is considered to be an exceptional member [1,2] of the family of iron (Fe)-based superconductors [3–7] for various reasons. First, FeSe is the structurally simplest of all members. It superconducts [8] below a critical temperature $T_c \approx 8$ K and $T_c$ can be significantly enhanced in thin films [9–12] and intercalated FeSe [13] or by pressure ($p$) [14–19]. Second, FeSe undergoes a structural transition [8,20,21] from a tetragonal to an orthorhombic state at $T_s \approx 90$ K at ambient $p$ which was shown to be nematic [22–25], i.e., driven by electronic degrees of freedom. In contrast to other Fe-based superconductors [26], the nematic transition in FeSe is not accompanied or closely followed by an antiferromagnetic transition [21,27]. Thus, it was suggested that FeSe represents an ideal platform to study a purely nematic phase and its interrelation with superconductivity [1]. Third, FeSe was found to be characterized by strong electronic correlations [28] leading to a small Fermi energy [2] which is comparable in size to the superconducting gap. This has recently raised the question whether FeSe is located deep in the crossover regime between weak-coupling BCS to strong-coupling BEC superconductivity [29–34]. The latter is characterized by superconducting fluctuations over a wide temperature ($T$) range above $T_c$.

The extent to which the properties of FeSe are comparable to those of other Fe-based superconductors has been strongly debated over the years [1]. In this regard, the study of the $T$-$p$ phase diagram [see Fig. 1(a)] yielded important new insights [27,35–47] (see Fig. S1). Above a characteristic pressure $p_1$, bulk magnetic order [27,43], which is likely stripe-type antiferromagnetic order [35,36,48], was observed below the magnetic transition temperature $T_M < T_s$ (i.e., the magnetic-nematic state). At even higher pressures, above a second characteristic pressure $p_2$, the magnetic-nematic ground state was found to be stabilized through a simultaneous first-order transition with $T_s = T_M$ [35,36,44]. This demonstrated that the phase diagram of FeSe at higher $p$ shows the same generic features in terms of the magnetic and structural transitions as other Fe-based superconductors, i.e., two subsequent, second-order phase transitions with $T_s > T_M$ that can be tuned to a simultaneous first-order transition ($T_s = T_M$) [35,36,44]. However, whether the purely nematic state at low pressures fits into this universal picture, is still a subject of debates [49–55].

With respect to the superconductivity of FeSe under pressure, there is an ongoing discussion about its nature. It was proposed early on that superconductivity exists over a

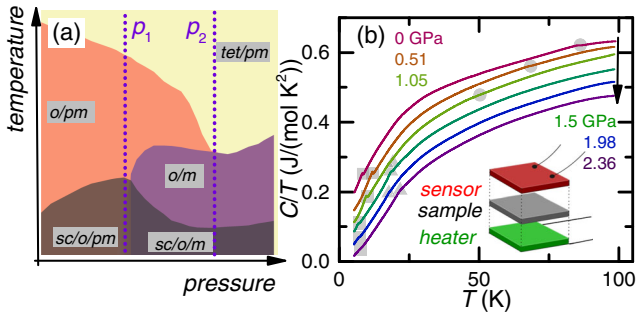


FIG. 1. (a) Schematic temperature-pressure phase diagram of FeSe, showing the extent of tetragonal (tet), orthorhombic (o), paramagnetic (pm), magnetic (m), and superconducting (sc) states and the two characteristic pressures $p_1$ and $p_2$ (see main text). (b) Selected specific heat data sets, $C/T$ vs $T$, at different pressures. Light grey regions indicate the position of the various anomalies detected by $C/T$, related to the structural (circles), the superconduting (squares), and the magnetic transition (triangles). The inset illustrates schematically the measurement configuration [56] to measure the specific heat under $p$.

 

wide $p$ range, i.e., in the purely nematic ($p < p_1$), but also in the magnetic-nematic $p$ range ($p > p_1$). In the latter regime, the simultaneous enhancement of $T_c$ and $T_M$ raised the idea of cooperative promotion of superconductivity and magnetism [43,57], contrary to other Fe-based superconductors. However, this scenario has not been substantiated to date, since microscopic probes, such as NMR [36], failed to detect any signature of superconductivity in the magnetic-nematic state for $p > p_2$. This has therefore even led to the question whether bulk superconductivity exists in FeSe for $p > p_2$ [36,58].

By studying the specific heat ($C$) under $p$ of a single crystal [59] of FeSe up to 2.36 GPa, we determine the full thermodynamic $T$-$p$ phase diagram of FeSe. We are therefore able to address various open issues related to superconductivity: our results confirm the bulk nature of superconductivity over the full $p$ range investigated, in particular also in the magnetic-nematic state for $p > p_2$. In this regime, our data suggest a competition of superconductivity and magnetism in FeSe. Even further, we argue that superconducting and magnetic fluctuations of temporal and/or spatial nature exist in FeSe at high $p$ over a wide range of temperatures above the respective bulk transition temperatures. These results therefore put FeSe in close similarity to the strongly correlated cuprate superconductors.

The specific heat of a vapor grown FeSe single crystal [59] was measured with an ac technique [see Fig. 1(b)] inside a liquid-medium piston-cylinder pressure cell in a home-built setup [56] (for more details, see the Supplemental Material [60]).

First, we focus on the $C$ data close to the structural and magnetic transitions at $T_s$ and $T_M$, respectively, in FeSe under $p$, as shown in Figs. 1(b) and 2 (and in Figs. S2–S7) to determine the characteristic pressures $p_1$ and $p_2$ from our experiment. $T_s$ is monotonically suppressed with increasing $p$ until it becomes indiscernible above 1.32 GPa (see Figs. 1(b) and S3). Magnetic ordering is observed in our data for $p \geq 0.91$ GPa [see Fig. 2(a) and Fig. S5 for low $p$ data]. This therefore defines $p_1$ in the $T$-$p$ phase diagram of FeSe (0.84 GPa $\leq p_1 \leq$ 0.91 GPa).

Upon increasing $p$, $T_M$ first increases steeply up to $\approx$1.2 GPa, then shows a slight reduction up to $\approx$1.9 GPa and then increases quickly for higher pressures. At the same time, the specific heat anomaly at $T_M$ [see Fig. 2(a)] evolves from a steplike shape, characteristic for second-order phase transitions at lower $p$, to a symmetric peak at higher $p$, which might be the result of a slightly broadened singularity of a first-order transition. This observation is therefore consistent with the picture [35,36] that the magnetic transition becomes first order close to where it merges with the structural transition. To define the characteristic pressure $p_2$ at which the character of the magnetic transition changes, we follow three complementary approaches. This includes measurements of the thermal

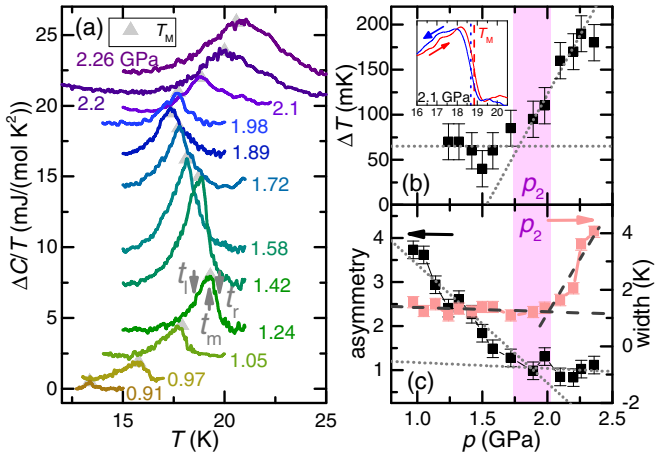


FIG. 2. (a) Specific heat anomaly of the magnetic transition at $T_M$, $\Delta C/T$, which is present for $p \geq 0.91$ GPa ($\sim p_1$) and obtained by subtracting a background from $C/T$ data. Data are offset for clarity. Faint, grey triangles indicate the position of $T_M$ in each data set. $t_l$, $t_m$, and $t_r$ are used to estimate asymmetry and width of the specific heat peak. (b) Hysteresis $\Delta T$ of $T_M$ between warming and cooling. Inset shows $d(C/T)/dT$ at 2.1 GPa upon warming and cooling. (c) Asymmetry (left axis) and width (right axis) of the specific heat peak at $T_M$. Dashed and dotted lines are guides to the eye, the purple bar indicates the position of the critical pressure range $p_2$.

hysteresis [see Fig. 2(b) and Fig. S7] and an analysis of the asymmetry and the width of the specific heat peak [see Fig. 2(c)]. We define the asymmetry as $(t_r - t_m/t_m - t_l)$, with $t_m$ ($t_r$ and $t_l$) being the temperatures at which the specific heat anomaly exhibits its maximum value (50% of the maximum value) and the width as $t_r - t_l$. All together, all three quantities exhibit a sudden change at $p_2 = (1.87 \pm 0.10)$ GPa.

Next, we present in Fig. 3 the evolution of the specific heat jump across the superconducting transition at $T_c$ in the three distinct pressure regimes (a) $p < p_1$, (b) $p_1 < p < p_2$, and (c) $p > p_2$ (see Figs. S8 and S9 for raw data). At all $p$ up to 2.36 GPa, we resolve a clear specific heat anomaly at low $T$, associated with the superconducting transition at $T_c$. To determine $T_c$ and the superconducting jump size $\Delta C_{sc}/T_c(p)$, we use an equal-area construction in $\Delta C/T$ [see dotted lines in inset of Fig. 3(a)]. For $p \lesssim p_1$, we find an increase of $T_c$ together with an increase of $\Delta C_{sc}/T_c$ [see Fig. 3(a)]. Soon after the onset of magnetism at $p_1$, $T_c$ and $\Delta C_{sc}/T_c$ are suppressed with $p$ for $p < p_2$. Above $p_2$, $T_c$ increases slowly, however, $\Delta C_{sc}/T_c$ continues to be monotonically suppressed with increasing $p$.

Remarkably, we also find a sudden change of the shape of the $\Delta C/T(T_c)$ anomaly from almost mean-field like for $p < p_1$ to a more $\lambda$-like shape with an extended high-$T$ tail for $p > p_1$. This change can be quantified in terms of a broadening parameter (see Fig. S10) which defines the width of superconducting transition and is shown in

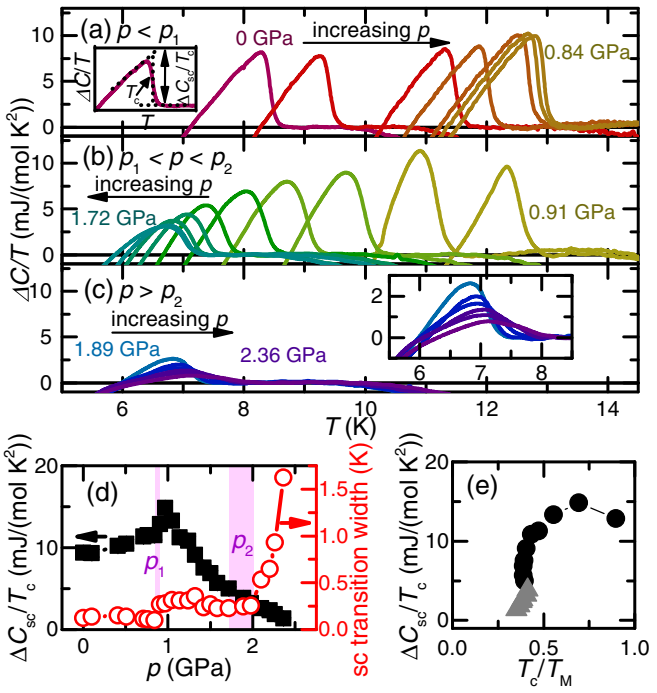


FIG. 3. (a)–(c) Estimate of the specific heat anomaly in FeSe at the superconducting transition, $\Delta C/T$, in the pressure regimes 0 GPa $\leq p \leq$ 0.84 GPa [$p < p_1$, (a)], 0.91 GPa $\leq p \leq$ 1.58 GPa [$p_1 < p < p_2$, (b)], and 1.72 GPa $\leq p \leq$ 2.36 GPa [$p > p_2$, (c)]. The inset of (c) shows a blow-up of the data set in the main panel. The dotted lines in the inset of (a) indicate exemplarily the equal-area construction in $\Delta C/T$ used to determine the superconducting jump size $\Delta C_{sc}/T_c$ and the critical temperature $T_c$. (d) Evolution of $\Delta C_{sc}/T_c$ (left axis) as well as superconducting transition width (right axis; see Fig. S10) as a function of $p$. Purple bars indicate the position of critical pressures $p_1$ and $p_2$. (e) $\Delta C_{sc}/T_c$ as a function of the ratio $T_c/T_M$. Black circles (grey triangles) correspond to data in the pressure regime $p_1 < p < p_2$ ($p > p_2$).

Fig. 3(d) (right axis): it is almost constant as a function of $p$ for $p < p_1$, then exhibits a clear jump at $p_1$ (see also Fig. S11) and levels off again, until it increases rapidly for $p > p_2$. We stress that such sudden changes in the broadening, as observed here at $p_1$ and *again* at $p_2$, are unlikely to result from pressure inhomogeneities related to the freezing of the pressure medium [61], and therefore rather reflect a change of intrinsic physics of FeSe.

We can now proceed with discussing the two central results of this study. The first one relates to the question of bulk superconductivity in FeSe under $p$ and its relationship with magnetism. Here, the observation of a finite $\Delta C_{sc}/T_c$ at all $p$ speaks in strong favor of bulk superconductivity in FeSe, which coexists with nematic order at low $p$ as well as with magnetic-nematic order at high $p$. The fact that $\Delta C_{sc}/T_c$, which, in simple BCS theory, is a measure of the superconducting condensation energy, is strongly suppressed with $p$ for $p \gtrsim p_1$ [see Fig. 3(d)] indicates that magnetism competes with superconductivity in FeSe, resulting in either microscopic coexistence or in a macroscopic phase segregation [62]. Importantly, competition is also the case for the region $p > p_2$, even though $T_c$ and $T_M$ both increase with $p$. This unusual possibility is included in an earlier model [63] on competing spin-density wave and superconducting order in itinerant systems, which provides the general tendency that competition leads to a decrease of $T_c/T_M$ (rather than a decrease of $T_c$ itself), when $T_M$ is increased. Our specific heat results of the bulk $T_M$ and $T_c$ values [see Figs. 4 and S1 (a)] indeed show that this is the case in FeSe at high $p$: notably, $\Delta C_{sc}/T_c$ is suppressed with decreasing $T_c/T_M$ [see Fig. 3(e)]. Therefore, our results strengthen the similarities of FeSe to other Fe-based superconductors [7,62,64,74–79].

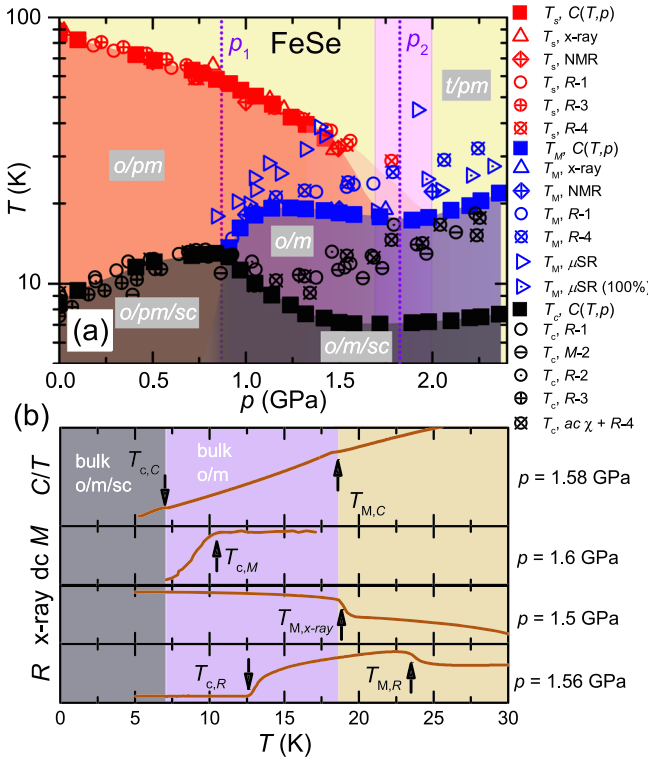


FIG. 4. (a) Temperature-pressure phase diagram of FeSe, determined from specific heat measurements $C(T,p)$ (full squares). Red symbols correspond to the structural transition temperature $T_s$, black symbols to the superconducting transition temperature $T_c$ and blue symbols to the magnetic transition temperature $T_M$. The phase regions are labeled by *t/pm* (tetragonal/paramagnetic; light yellow), *o/pm* (orthorhombic/paramagnetic; red), *o/m* (orthorhombic/magnetic; blue) and *sc* (superconducting; brown/grey). Purple dotted vertical lines mark two characteristic pressures, $p_1$ and $p_2$. The error in the determination of $p_2$ is indicated by the light purple bar. The specific heat data are contrasted with data from various other techniques from literature, i.e., x-ray scattering [35], NMR [37], resistance, and magnetization (*R*-1 [38], *R*-2 [39], and *M*-2 [39], *R*-3 [40], *R*-4 [41]), and $\mu$SR [43,44]. (b) Comparison of $C/T$ data at 1.58 GPa to *M* [39] data, x-ray data of the orthorhombic distortion [35], and *R* [38] (*R*) data at similar nominal pressures.

The second result is summarized in the $T$-$p$-phase diagram in Fig. 4(a) (see Fig. S1 for simplified versions of this phase diagram). In this figure, we compare the transition temperatures $T_s$, $T_M$, and $T_c$ from the present $C(T,p)$ work (full symbols), with those reported in the literature [80], based on x-ray scattering [35,45], NMR [37], resistance [38–41], magnetization [41], and $\mu$SR [43,44] (open symbols). Surprisingly, whereas the majority of $T_s$ values and $T_c$ values for $p < p_1$, as well as the $p_1$ values themselves, are rather consistent, the $T_M$ and $T_c$ values for $p > p_1$ show strong discrepancies. Given that specific heat measurements provide the bulk, thermodynamic (and static) transition temperatures, we suggest below one possible way to rationalize these findings is in terms of superconducting and magnetic fluctuations which exist for $p \geq p_1$ over a wide $T$ range above $T_c$ and $T_M$, respectively.

In terms of superconductivity for $p > p_1$, not only is the discrepancy of bulk $T_c$ values from the present study ($T_{c,C}$) and those from previous reports from transport and susceptibility [$T_{c,R/\chi} \gg T_{c,C}$, Figs. 4(a) and 4(b)] remarkable, but it must be recalled that there is a simultaneous, sudden change in the shape of the $C$ anomaly at $p_1$, depicted in Fig. 3. A sudden increase in broadening of the feature at $T_c$ at $p_1$ was also observed in other quantities [41,57], such as resistance, despite being much larger there. Contrary to changes in transport features, though, the observed change in the specific heat feature is considered as a well-established signature [65,81,82] of superconducting fluctuations [30] above the mean-field $T_c$. In this situation, the onset of diamagnetism [31,82] at $T_{c,\chi}$ is likely found at higher temperatures than the bulk $T_{c,C}$, consistent with our results. Revisiting susceptibility data [39,41] demonstrates that the bulk $T_{c,C}$ actually corresponds to the temperature at which FeSe exhibits saturating diamagnetism [see Fig. 4(b)]. Thus, a comparison of onset $T_{c,\chi}$ and $T_{c,C}$ can be used to estimate the $T$ range in which superconducting fluctuations exist. This $T$ range is small, but present for $p_1 < p < p_2$ and it increases rapidly above $p_2$ ($\approx 10$ K $\simeq 2T_c$ at 2.36 GPa, see Figs. 4, S1, and S13). This mirrors the observed broadening of the $\Delta C/T$ feature at $T_c$. Taken together, all these observations are consistent with a picture, in which significant changes of the Fermi surface [38,83,84] at $p_1$ and $p_2$ increase the $T$ range of fluctuations. Such extended fluctuations in the presence of competing magnetic order, suggested in the present work, might also naturally account for the absence of pronounced features at $T_c$ in microscopic NMR data [36] for $p > p_2$.

Concerning the magnetic transition, we find that the $T_M$ values from $C(T,p)$ are at the lower bound of values reported so far. It is remarkable, though, that similar $T_M$ values were inferred using the same technique in different studies (see, e.g., the two sets of open blue circles from resistance studies in Fig. 4). This argues against experimental artifacts arising from a combination of different samples with slightly different stochiometry and different pressure media being solely responsible for the discrepancy in $T_M$ values. Instead, it seems likely that the observed spread in $T_M$ is related to the time scale of each experiment, ranging from $\sim\mu$s for $\mu$SR [43,44] up to $\sim$seconds for NMR [36,37] up to static for $C(T)$ and x-ray probes (measuring the increase of orthorhombicity associated with the development of long-range order [35]). We refrain from including the $T_M$ values inferred from the resistance in the present discussion, as the associated time scale, given by the scattering time, cannot be unequivocally defined. As $T_M(p)$ from the two static probes [$C(T)$ and x-ray] fall on top of each other [$T_{M,C} \simeq T_{M,\mathrm{x\,ray}}$, see Figs. 4(b) and S1 (b)] and $T_{M,C} \lesssim T_{M,\mathrm{NMR}} \lesssim T_{\mu\mathrm{SR}}$ at any given $p$, this is highly suggestive of magnetic fluctuations existing far above the static $T_{M,C}$. The extent in $T$ of these fluctuations above $T_M$ can be estimated from the spread of transition temperatures in Fig. 4. This spread increases upon increasing $p$, even more rapidly above $p_2$, and reaches more than $\approx$30 K above 2 GPa. The width of the specific heat peak at $T_M$ [see Fig. 2(c)] provides further support for this statement, as it shows a progressive increase above $p_2$ (see Fig. S12), which reflects a sizable loss of magnetic entropy preceding the bulk $T_{M,C}$ upon cooling.

Another scenario which could give rise to a similar phenomenology of the $T$-$p$ phase diagram, as well as the specific heat features, invokes electronic inhomogeneity [85] giving rise to a spatially fluctuating state. It is important to note though, that this inhomogeneity then must be intrinsically induced by the occurrence of magnetism, as evident from our phase diagram in Fig. 4. It could, e.g., arise from the formation of domains in the magnetically ordered state which are pinned by extrinsic disorder, inevitable in any real crystal. Whereas such a scenario certainly promotes a nonbulk superconducting state above $T_c$, causing zero resistance well above the bulk $T_c$ (such as the recently proposed fragile superconducting state [86]), it unlikely explains the correlation of time scales and transition temperatures for the magnetic transition. Thus, whereas for the superconducting transition either temporal or spatial fluctuations are consistent with our data, the results speak in favor of a temporal nature of the magnetic fluctuations.

To verify which of these two scenarios is applicable in FeSe, it will be of crucial importance to identify the characteristic energy scales of the different orders in FeSe under pressure. One important key question here will be to resolve the magnetic structure of FeSe for $p > p_1$ which has still not been unequivocally determined to date. Nevertheless, we want to stress that our picture of the $T$-$p$ phase diagram of FeSe presents close similarity to the ones of the high-$T_c$ cuprate superconductors [87]. In the latter case, there is growing evidence for the coexistence of superconductivity in the underdoped regime with other competing phases, such as charge-density waves [88]

enhancing fluctuations [89,90] associated with both orders over a wide $T$ range above the respective bulk transition temperatures [87,91]. Whereas this comparison is purely phenomenological at present, FeSe might serve as an important reference system to investigate the origin of such extended fluctuating regimes in the presence of competing orders, as superconductivity can be tuned through nonmagnetic and magnetic states solely via pressure which does not introduce any additional disorder.

In conclusion, the presented specific heat data demonstrate that superconductivity is bulk in FeSe up to 2.36 GPa, and competes with magnetism, whenever present. In the presence of magnetism, our results strongly suggest that superconducting and magnetic fluctuations exist over a wide temperature range above the respective bulk transition temperatures. This puts the phase diagram of FeSe under pressure in close similarity to those of underdoped cuprates in which the enhancement of phase fluctuations due to competing orders is considered as a key ingredient for high-$T_c$ superconductivity.

We thank A. Kreyssig (Kreyßig), V. G. Kogan, D. Ryan, and B. Andersen for useful discussions. In addition, we thank G. Drachuck for useful discussions and technical support with the ac specific heat setup in the initial stages of this work. Work at the Ames Laboratory was supported by the U.S. Department of Energy, Office of Science, Basic Energy Sciences, Materials Sciences and Engineering Division. The Ames Laboratory is operated for the U.S. Department of Energy by Iowa State University under Contract No. DEAC02-07CH11358.

*Corresponding author.
egati@ameslab.gov
†Present address: Institute for Solid State Physics, Karlsruhe Institute of Technology, 76021 Karlsruhe, Germany.

[1] A. E. Böhmer and A. Kreisel, J. Phys. Condens. Matter **30**, 023001 (2018).
[2] A. I. Coldea and M. D. Watson, Annu. Rev. Condens. Matter Phys. **9**, 125 (2018).
[3] J. Paglione and R. L. Greene, Nat. Phys. **6**, 645 (2010).
[4] D. C. Johnston, Adv. Phys. **59**, 803 (2010).
[5] G. R. Stewart, Rev. Mod. Phys. **83**, 1589 (2011).
[6] H. Hosono and K. Kuroki, Physica (Amsterdam) **514C**, 399 (2015).
[7] P. C. Canfield and S. L. Bud'ko, Annu. Rev. Condens. Matter Phys. **1**, 27 (2010).
[8] F.-C. Hsu *et al.*, Proc. Natl. Acad. Sci. U.S.A. **105**, 14262 (2008).
[9] J.-F. Ge, Z.-L. Liu, C. Liu, C.-L. Gao, D. Qian, Q.-K. Xue, Y. Liu, and J.-F. Jia, Nat. Mater. **14**, 285 (2015).
[10] M. V. Sadovskii, Phys. Usp. **59**, 947 (2016).
[11] Z. Wang, C. Liu, Y. Liu, and J. Wang, J. Phys. Condens. Matter **29**, 153001 (2017).
[12] D. Huang and J. E. Hoffman, Annu. Rev. Condens. Matter Phys. **8**, 311 (2017).
[13] M. Burrard-Lucas *et al.*, Nat. Mater. **12**, 15 (2013).
[14] Y. Mizuguchi, F. Tomioka, S. Tsuda, T. Yamaguchi, and Y. Takano, Appl. Phys. Lett. **93**, 152505 (2008).
[15] S. Medvedev *et al.*, Nat. Mater. **8**, 630 (2009).
[16] S. Margadonna, Y. Takabayashi, Y. Ohishi, Y. Mizuguchi, Y. Takano, T. Kagayama, T. Nakagawa, M. Takata, and K. Prassides, Phys. Rev. B **80**, 064506 (2009).
[17] G. Garbarino, A. Sow, P. Lejay, A. Sulpice, P. Toulemonde, M. Mezouar, and M. Núñez-Regueiro, Europhys. Lett. **86**, 27001 (2009).
[18] S. Masaki, H. Kotegawa, Y. Hara, H. Tou, K. Murata, Y. Mizuguchi, and Y. Takano, J. Phys. Soc. Jpn. **78**, 063704 (2009).
[19] H. Okabe, N. Takeshita, K. Horigane, T. Muranaka, and J. Akimitsu, Phys. Rev. B **81**, 205119 (2010).
[20] S. Margadonna, Y. Takabayashi, M. T. McDonald, K. Kasperkiewicz, Y. Mizuguchi, Y. Takano, A. N. Fitch, E. Suard, and K. Prassides, Chem. Commun. (Cambridge) 5607 (2008).
[21] T. M. McQueen, A. J. Williams, P. W. Stephens, J. Tao, Y. Zhu, V. Ksenofontov, F. Casper, C. Felser, and R. J. Cava, Phys. Rev. Lett. **103**, 057002 (2009).
[22] A. E. Böhmer, T. Arai, F. Hardy, T. Hattori, T. Iye, T. Wolf, H. v. Löhneysen, K. Ishida, and C. Meingast, Phys. Rev. Lett. **114**, 027001 (2015).
[23] M. D. Watson *et al.*, Phys. Rev. B **91**, 155106 (2015).
[24] M. A. Tanatar *et al.*, Phys. Rev. Lett. **117**, 127001 (2016).
[25] S.-H. Baek, D. V. Efremov, J. M. Ok, J. S. Kim, J. van den Brink, and B. Büchner, Nat. Mater. **14**, 210 (2015).
[26] R. M. Fernandes, A. V. Chubukov, and J. Schmalian, Nat. Phys. **10**, 97 (2014).
[27] M. Bendele, A. Amato, K. Conder, M. Elender, H. Keller, H.-H. Klauss, H. Luetkens, E. Pomjakushina, A. Raselli, and R. Khasanov, Phys. Rev. Lett. **104**, 087003 (2010).
[28] M. Yi *et al.*, Nat. Commun. **6**, 7777 (2015).
[29] S. Kasahara *et al.*, Proc. Natl. Acad. Sci. U.S.A. **111**, 16309 (2014).
[30] S. Kasahara *et al.*, Nat. Commun. **7**, 12843 (2016).
[31] T. Watashige *et al.*, J. Phys. Soc. Jpn. **86**, 014707 (2017).
[32] S. Rinott, K. B. Chashka, A. Ribak, E. D. L. Rienks, A. Taleb-Ibrahimi, P. L. Fevre, F. Bertran, M. Randeria, and A. Kanigel, Sci. Adv. **3**, e1602372 (2017).
[33] T. Hanaguri, S. Kasahara, J. Böker, I. Eremin, T. Shibauchi, and Y. Matsuda, Phys. Rev. Lett. **122**, 077001 (2019).
[34] Y. Lubashevsky, E. Lahoud, K. Chashka, D. Podolsky, and A. Kanigel, Nat. Phys. **8**, 309 (2012).
[35] K. Kothapalli *et al.*, Nat. Commun. **7**, 12728 (2016).
[36] P. S. Wang, S. S. Sun, Y. Cui, W. H. Song, T. R. Li, R. Yu, H. Lei, and W. Yu, Phys. Rev. Lett. **117**, 237001 (2016).
[37] P. Wiecki, M. Nandi, A. E. Böhmer, S. L. Bud'ko, P. C. Canfield, and Y. Furukawa, Phys. Rev. B **96**, 180502(R) (2017).
[38] U. S. Kaluarachchi, V. Taufour, A. E. Böhmer, M. A. Tanatar, S. L. Bud'ko, V. G. Kogan, R. Prozorov, and P. C. Canfield, Phys. Rev. B **93**, 064503 (2016).
[39] K. Miyoshi, K. Morishita, E. Mutou, M. Kondo, O. Seida, K. Fujiwara, J. Takeuchi, and S. Nishigori, J. Phys. Soc. Jpn. **83**, 013702 (2014).

[40] S. Knöner, D. Zielke, S. Köhler, B. Wolf, T. Wolf, L. Wang, A. Böhmer, C. Meingast, and M. Lang, Phys. Rev. B **91**, 174510 (2015).
[41] T. Terashima *et al.*, J. Phys. Soc. Jpn. **84**, 063701 (2015).
[42] J. P. Sun *et al.*, Nat. Commun. **7**, 12146 (2016).
[43] M. Bendele, A. Ichsanow, Y. Pashkevich, L. Keller, T. Strässle, A. Gusev, E. Pomjakushina, K. Conder, R. Khasanov, and H. Keller, Phys. Rev. B **85**, 064517 (2012).
[44] R. Khasanov, R. M. Fernandes, G. Simutis, Z. Guguchia, A. Amato, H. Luetkens, E. Morenzoni, X. Dong, F. Zhou, and Z. Zhao, Phys. Rev. B **97**, 224510 (2018).
[45] A. E. Böhmer *et al.*, Phys. Rev. B **100**, 064515 (2019).
[46] V. Svitlyk, M. Raba, V. Dmitriev, P. Rodière, P. Toulemonde, D. Chernyshov, and M. Mezouar, Phys. Rev. B **96**, 014520 (2017).
[47] B. W. Lebert, V. Balédent, P. Toulemonde, J. M. Ablett, and J.-P. Rueff, Phys. Rev. B **97**, 180503(R) (2018).
[48] R. Khasanov, Z. Guguchia, A. Amato, E. Morenzoni, X. Dong, F. Zhou, and Z. Zhao, Phys. Rev. B **95**, 180504(R) (2017).
[49] A. V. Chubukov, M. Khodas, and R. M. Fernandes, Phys. Rev. X **6**, 041045 (2016).
[50] J. K. Glasbrenner, I. I. Mazin, H. O. Jeschke, R. M. F. P. J. Hirschfeld, and R. Valentí, Nat. Phys. **11**, 953 (2015).
[51] S. Onari, Y. Yamakawa, and H. Kontani, Phys. Rev. Lett. **116**, 227001 (2016).
[52] Y. Yamakawa, S. Onari, and H. Kontani, Phys. Rev. X **6**, 021032 (2016).
[53] A. V. Chubukov, R. M. Fernandes, and J. Schmalian, Phys. Rev. B **91**, 201105(R) (2015).
[54] R. Yu and Q. Si, Phys. Rev. Lett. **115**, 116401 (2015).
[55] F. Wang, S. A. Kivelson, and D.-H. Lee, Nat. Phys. **11**, 959 (2015).
[56] E. Gati, G. Drachuck, L. Xiang, L.-L. Wang, S. L. Bud'ko, and P. C. Canfield, Rev. Sci. Instrum. **90**, 023911 (2019).
[57] G.-Y. Chen, E. Wang, X. Zhu, and H.-H. Wen, Phys. Rev. B **99**, 054517 (2019).
[58] K. Y. Yip, Y. C. Chan, Q. Niu, K. Matsuura, Y. Mizukami, S. Kasahara, Y. Matsuda, T. Shibauchi, and S. K. Goh, Phys. Rev. B **96**, 020502(R) (2017).
[59] A. E. Böhmer, V. Taufour, W. E. Straszheim, T. Wolf, and P. C. Canfield, Phys. Rev. B **94**, 024526 (2016).
[60] See Supplemental Material at http://link.aps.org/supplemental/10.1103/PhysRevLett.123.167002 for description of experiment, simplified versions of the temperature-pressure phase diagram and additional specific heat data on larger temperature scales, which includes Refs. [30,35,37–39,41–43,59,61–73].
[61] M. S. Torikachvili, S. K. Kim, E. Colombier, S. L. Bud'ko, and P. C. Canfield, Rev. Sci. Instrum. **86**, 123904 (2015).
[62] S. C. Cheung *et al.*, Phys. Rev. B **97**, 224508 (2018).
[63] K. Machida, J. Phys. Soc. Jpn. **50**, 2195 (1981).
[64] S. L. Bud'ko, V. G. Kogan, R. Prozorov, W. R. Meier, M. Xu, and P. C. Canfield, Phys. Rev. B **98**, 144520 (2018).
[65] H. Yang, G. Chen, X. Zhu, J. Xing, and H.-H. Wen, Phys. Rev. B **96**, 064501 (2017).
[66] F. Hardy *et al.*, Phys. Rev. B **99**, 035157 (2019).
[67] A. Muratov, A. Sadakov, S. Gavrilkin, A. Prishchepa, G. Epifanova, D. Chareev, and V. Pudalov, Physica B (Amsterdam) **536**, 785 (2018).
[68] Y. Sun, S. Kittaka, S. Nakamura, T. Sakakibara, K. Irie, T. Nomoto, K. Machida, J. Chen, and T. Tamegai, Phys. Rev. B **96**, 220505 (2017).
[69] S. K. Kim, M. S. Torikachvili, E. Colombier, A. Thaler, S. L. Bud'ko, and P. C. Canfield, Phys. Rev. B **84**, 134525 (2011).
[70] B. Bireckoven and J. Wittig, J. Phys. E **21**, 841 (1988).
[71] W. R. Meier *et al.*, npj Quantum Mater. **3**, 5 (2018).
[72] A. Kreyssig *et al.*, Phys. Rev. B **97**, 224521 (2018).
[73] L. Xiang, W. R. Meier, M. Xu, U. S. Kaluarachchi, S. L. Bud'ko, and P. C. Canfield, Phys. Rev. B **97**, 174517 (2018).
[74] M. Rotter, M. Tegel, I. Schellenberg, F. M. Schappacher, R. Pöttgen, J. Deisenhofer, A. Günther, F. Schrettle, A. Loidl, and D. Johrendt, New J. Phys. **11**, 025014 (2009).
[75] D. K. Pratt, W. Tian, A. Kreyssig, J. L. Zarestky, S. Nandi, N. Ni, S. L. Bud'ko, P. C. Canfield, A. I. Goldman, and R. J. McQueeney, Phys. Rev. Lett. **103**, 087001 (2009).
[76] A. D. Christianson, M. D. Lumsden, S. E. Nagler, G. J. MacDougall, M. A. McGuire, A. S. Sefat, R. Jin, B. C. Sales, and D. Mandrus, Phys. Rev. Lett. **103**, 087002 (2009).
[77] H. Luo *et al.*, Phys. Rev. Lett. **108**, 247002 (2012).
[78] R. M. Fernandes and J. Schmalian, Phys. Rev. B **82**, 014521 (2010).
[79] A. E. Böhmer, F. Hardy, L. Wang, T. Wolf, P. Schweiss, and C. Meingast, Nat. Commun. **6**, 7911 (2015).
[80] We omit data points of Refs. [36,42] due to pressure offsets, and Ref. [39] due to a different criterion for $T_s$.
[81] A. Junod, A. Erb, and C. Renner, Physica (Amsterdam) **317-318C**, 333 (1999).
[82] K. Adachi and R. Ikeda, Phys. Rev. B **96**, 184507 (2017).
[83] T. Terashima *et al.*, Phys. Rev. B **93**, 094505 (2016).
[84] P. Massat *et al.*, Phys. Rev. Lett. **121**, 077001 (2018).
[85] J. H. J. Martiny, A. Kreisel, and B. M. Andersen, Phys. Rev. B **99**, 014509 (2019).
[86] Y. Yu and S. A. Kivelson, Phys. Rev. B **99**, 144513 (2019).
[87] B. Keimer, S. A. Kivelson, M. R. Norman, S. Uchida, and J. Zaanen, Nature (London) **518**, 179 (2015).
[88] E. H. da Silva Neto *et al.*, Science **343**, 393 (2014).
[89] S. A. Kivelson, I. P. Bindloss, E. Fradkin, V. Oganesyan, J. M. Tranquada, A. Kapitulnik, and C. Howald, Rev. Mod. Phys. **75**, 1201 (2003).
[90] D. H. Torchinsky, F. Mahmood, A. T. Bollinger, I. Božović, and N. Gedik, Nat. Mater. **12**, 387 (2013).
[91] I. M. Vishik, Rep. Prog. Phys. **81**, 062501 (2018).